

A Parallel-plate Capacitor-Effect in Earth's Dayside Ionosphere

Magnus F Ivarsen, Jean-Pierre St-Maurice,* Glenn C Hussey, and Kathryn McWilliams
Department of Physics and Engineering Physics, University of Saskatchewan, Saskatoon, Canada

Yaqi Jin and Lasse B N Clausen
Department of Physics, University of Oslo, Oslo, Norway

Devin R Huyghebaert[†]
Department of Physics and Technology, UiT The Arctic University of Norway, Tromsø, Norway

Yukinaga Miyashita[‡]
Space Science Division, Korea Astronomy and Space Science Institute, Daejeon, South-Korea

David Sibeck
Goddard Space Flight Center, NASA, Greenbelt, USA
 (Dated: January 9, 2025)

During the 23 April 2023 geospace storm, we observed chorus wave-driven energetic particle precipitation on closed magnetic field lines in the dayside magnetosphere. Simultaneously and in the ionosphere's bottom-side, we observed signatures of impact ionization and strong enhancements in the ionospheric electric field strength, via radar-detection of meter-scale turbulence, and with matching temporal characteristics as that of the magnetospheric observations (correlation coefficient = 0.78). During geospace storms, then, turbulent structuring as well as fast electrodynamics in the dayside polar ionosphere can be driven by wave-particle interactions in the magnetosphere.

I. INTRODUCTION

The solar wind, a stream of plasma at various densities, pushes against Earth's magnetosphere, driving large-scale electrical currents and plasma convection in Earth's ionosphere [1], ultimately brought about by magnetic reconnection, the interface between the terrestrial and solar magnetic fields. The process transfers magnetic flux from the dayside to the nightside [2]. On the Sun-facing side of the magnetosphere, closed field-lines open up to the solar wind, forming the magnetospheric cleft, or *cusp* region [3], which plays host to plasma outflow and particle precipitation [4, 5].

Poleward-moving auroral forms are frequently sighted in the ionospheric cusp, and are manifestations of dayside magnetic reconnection. They consist mostly of red auroral arcs that drift poleward along with the reconnected field-lines from the cusp and into the polar cap *in pulses* [6–8], as is illustrated in Figure 1a). The pulsations reflect the temporal evolution in flux transfer events, meaning that a study of the dynamics in one system is applicable to the other [9, 10]. For this reason, the study of poleward-moving auroral forms have yielded crucial physical insight into the magnetosphere. Relevant for the study at hand, such aurorae are invariably accom-

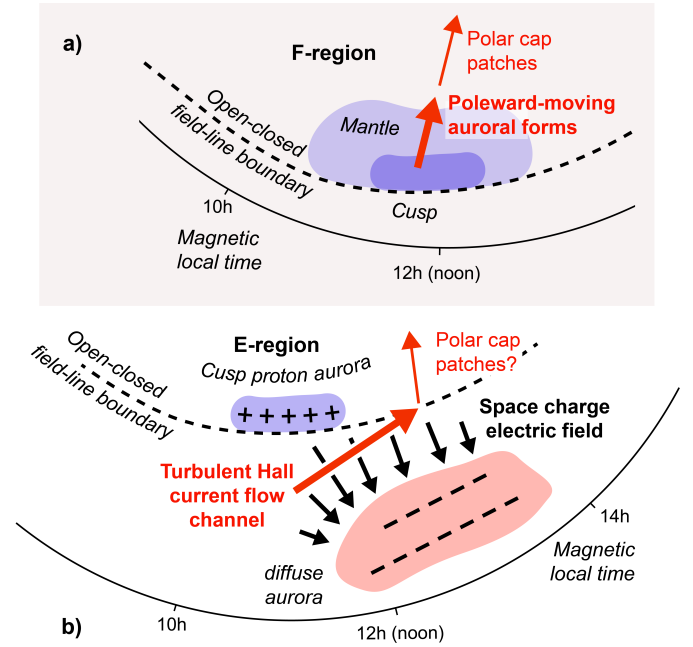


FIG. 1. **Panel a)**: Schematic drawing of the cusp at an altitude of 350 km, showing the cusp, its extended mantle, and the motion of traditional poleward-moving aurora forms. **Panel b)**: Schematic drawing of the dayside ionosphere at an altitude of 100 km, showing the impact of the cusp proton aurora, as well as a high-energy diffuse aurora. The two regions are separated by the open-closed field-line boundary and act akin to a parallel-plate capacitor. The action may push islands of ionization into the polar cap, if aided by day-side reconnection.

* Also at Department of Physics and Astronomy, University of Western Ontario, London, Ontario, Canada

[†] Also at Department of Physics and Engineering Physics, University of Saskatchewan, Saskatoon, Canada

[‡] Also at Department of Astronomy and Space Science, Korea University of Science and Technology, Daejeon, South-Korea

panied by fast plasma flow channels in the topside ionosphere [11, 12], with typical reported speeds ranging from 500 m/s to 2 km/s [13].

There are however observations of poleward-moving forms that move faster than the magnetospheric convection would imply [14], in counter-intuitive directions [15], and some that occur on *closed* magnetic field-lines [16], observations that challenge the accepted notion of magnetic flux being peeled off from the magnetopause into the polar cap [17]. In an attempt at reconciling the field, Ref. [18] proposed that hot electrons from a dayside plasma sheet [19] may precipitate in numbers sufficient to produce a perturbation electric field that powers fast poleward drift, a situation that we illustrate in Figure 1b).

Indeed, high-energy diffuse aurorae are a staple of the dayside ionosphere [20–22], where the mechanisms responsible originate with chorus waves (and other waves) near the magnetospheric equator; these cause pitch-angle scattering of the local electron population into the loss cone, and subsequent precipitation into Earth’s atmosphere [23, 24]. Having high kinetic energy, dayside diffuse aurorae will ionize the E-region, the bottomside ionosphere [25], at altitudes even lower than the extant extreme ultra-violet radiation from Sun would imply [26].

The above paragraphs describes the energy source for the mechanism suggested by Ref. [18], and the resulting fast motions are found in recent radar measurements of fast-moving electric field structures in the E-region ionosphere [27]. Figure 1b) presents a schematic of the process, and thereby summarizes the results of Ref. [27] and the present letter: On the north-eastern flank of a region containing diffuse aurorae, a series of super-fast turbulent Hall flow channels manifested. Given the proximity to the ion precipitation inside the cusp, an experiment akin to a parallel-plate capacitor emerges. Aided by dayside reconnection, the action may in the end transport plasma into the polar cap, thereby seeding polar cap patches.

Since dynamic and active aurorae dissipate energy, the question of what powers them strikes at the heart of the ionosphere-magnetosphere coupling; the greater energy flow from the solar wind down to Earth’s dense resistor of an ionosphere. Whereas traditional poleward-moving auroral forms are powered directly by the coupling between the cusp and the solar wind, we here evoke a mechanism involving oscillatory magnetic energy and the particle populations near the magnetospheric equator. In particular, whistler-mode chorus waves are the ultimate source of free energy in the system under study (a bold claim that is substantiated in a companion paper [27]).

The dataset used in the present letter consists of coherent radar echoes from the unstable E-region, also called the radar aurora [29]. In the companion paper, Ref. [27], we present in detail observations of dynamic radar aurorae that would seem to drift poleward but mostly eastward, at a location equatorward of the cusp and on closed magnetic field-lines, measured using the ICEBEAR radar. ICEBEAR is a coherent-scatter radar [30] whose signal re-

flects off small (3 meters) Farley-Buneman Waves, unstable structures excited by the relative motion between electrons and ions [31, 32]. The small-scale turbulence dissipates fast, giving the radar aurora an ephemeral quality. The apparent motion of the radar aurorae therefore measure the ionospheric electric field [33, 34].

Based on such electric field observations through a one-hour interval during the onset of the 23 April 2023 geomagnetic storm, the present letter substantiates a series of transient, turbulent Hall currents that formed on the poleward side of dayside diffuse aurorae. In the companion paper, Ref. [27], we demonstrate that chorus-wave-driven particle precipitation from the equatorial magnetopause were ultimately responsible for producing these turbulent Hall currents, and we infer a parallel-plate capacitor-effect forming against proton precipitation in the ionospheric cusp.

II. RESULTS

Figure 2 elucidates the state of the solar wind prior to the 23 April 2023-storm (panels a, b), and then summarizes the findings of our companion paper (panels c, d). Our observations were made in full daylight around noon during the geomagnetic storm’s main phase. At 17:35 UT the Sym-H index registered a storm sudden commencement (Figure 2b), as well as intense pressure oscillations, indicative of non-linear processes near the magnetosheath, such as bow shock ripples and high-speed jets [35], a source of free energy for the dayside ionosphere on closed field-lines [36]. The action is followed by a severe southward turn of the interplanetary magnetic field, with $B_Z < -20$ nT sustained for around 2.5 hours starting from around 18:30 UT (Figure 2a). This enabled an extreme equatorward shift of the auroral oval [37]. Further, a dense, storm-enhanced plume of plasma originating near the equator drifted poleward along the entire dayside northern hemisphere [38], and the interval between 19 UT and 23 UT saw equatorial plasma bubbles reaching sub-auroral latitudes [39].

Figure 2c summarizes the various velocities measured during the one-hour interval between 18:30 UT and 19:30 UT over Rabbit Lake, in Canada. Measurements from SuperDARN are plotted in red and green, utilizing (F-region) data both from a local radar and inferred from the global convection model respectively. In blue circle datapoints we show the ICEBEAR velocities, which are the motions of E-region radar aurorae, as they appear and disappear inside of the radar’s field-of-view. We note that the ICEBEAR velocities often exceed 2000 m/s in magnitude, and are generally much higher in magnitude than the SuperDARN-measured F-region drifts.

It is important to note that the bulk motion of plasma structures in the E-region has long been poorly understood. Individual turbulent structures generally do not move faster than the local ion sound speed, that is, the zero-growth condition for the Farley-Buneman instability

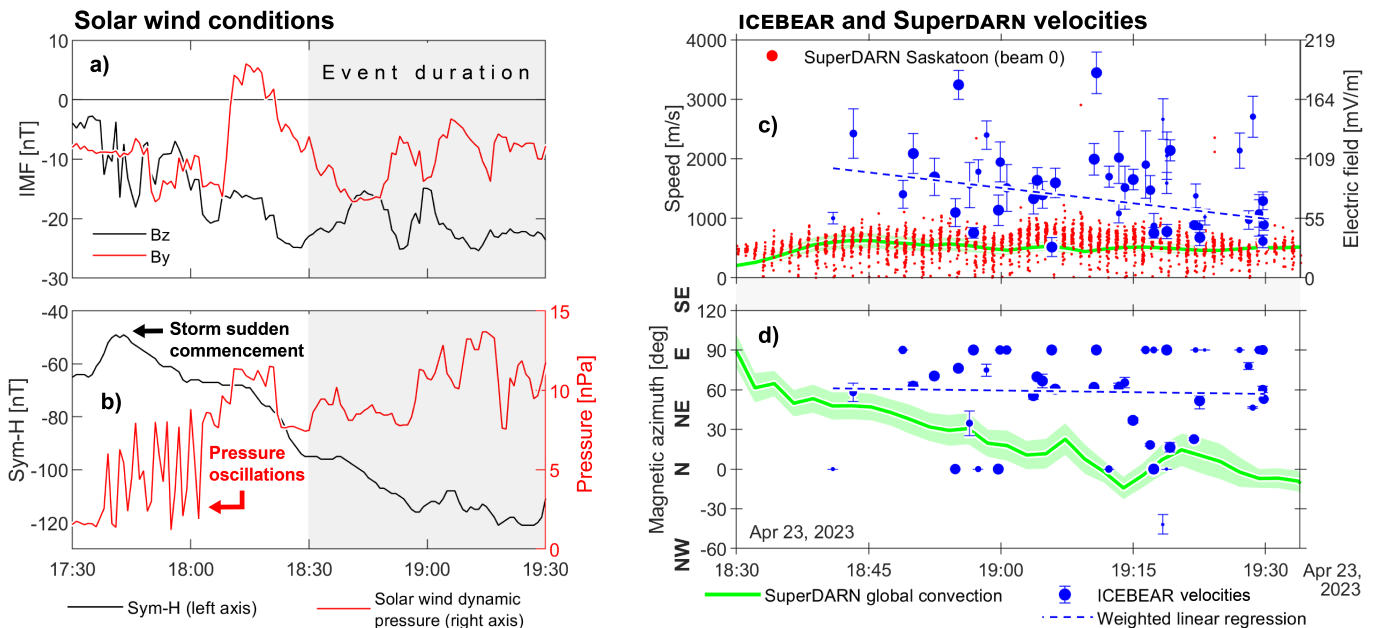


FIG. 2. **Panels a) and b):** Solar wind parameters and geomagnetic activity index for the interval 17:30 UT – 19:30 UT on 23 April 2023, with a shaded gray area denoting the duration of the event under study. Panel a) shows the interplanetary magnetic field B_z (black) and B_y (red) components timeshifted to the bowshock [28]. Panel b) shows the Sym-H geomagnetic storm index (black, left axis) and the solar wind dynamic pressure (red, right axis). **Panels c) and d)** show the apparent motions of 48 ICEBEAR 3D echo clusters that were detected and tracked between 18:30 UT and 19:30 UT on 23 April 2023 (blue datapoints). Clusters are selected for containing a minimum of 300 echoes, a minimum duration of 6 seconds, as well as variability that did not exceed 2/3 of the cluster speed itself. Panel c) shows speed while panel d) shows the direction (magnetic azimuth, or the angle with respect to magnetic north). Circle points represent individual clusters with sizes reflecting the number of echoes contained in each cluster. Blue errorbars denote mean variability, in the form of 68-percent confidence intervals of the linear fits of the echo cluster motion measurements. Dashed blue lines give weighted linear regressions in time. Thick green lines give the corresponding observations deduced from the SuperDARN global convection maps, both for speed (c) and direction (d), with the shaded green area denoting a single standard deviation from the mean. Doppler shifts measured by the Saskatoon SuperDARN radar are shown in red dots (using beam 0, which is roughly poleward). The right y -axis in panel c) shows the electric field strength inferred from the motions, using $E = v/B$.

[40, 41]. A value of around 300 m/s – 600 m/s is favoured. A recent paper, Ref. [34], interprets the much faster *apparent* motion of radar aurorae as being caused by the ephemeral nature of small-scale plasma turbulence: when the instability drivers (electric field enhancements) move, new turbulent waves are continuously excited along their paths, with each turbulent wave quickly saturating and dissipating. The apparent radar motions, or ‘echo bulk motions’, act as proxy measurements of the ionospheric electric field [33, 34].

The direct implication of Refs. [33, 34] are that the disproportionately fast ICEBEAR velocities in Figure 2c) are caused by highly localized electric field structures, capable of saturating the Farley-Buneman instability.

Figure 3 adds to this one-sentence summary with total-electron-content (TEC) measurements derived from a distributed network of ground-based GNSS receivers. This quantity is considered a height-integrated (column) density of plasma in the ionosphere. In Figure 3, TEC values are shown with blue contour lines of constant TEC. Global (modelled) SuperDARN convection velocities are superposed as a network of magenta arrows.

A green vector field shows the spatially and temporally averaged ICEBEAR velocities. Panel a) integrates over 11 minutes during the flyover of NOAA-18, a United States weather satellite that confirmed the location of the ionospheric cusp (see Figure 2 in Ref. [27]). Panel b) integrates over a 35-minute period that encompasses a conjunction with the inner-magnetosphere spacecraft Arase, whose data confirms the presence of diffuse aurorae. The latter two statements carry a heavy weight and are substantiated in the companion paper [27].

Transient, turbulent Hall currents

Based on the two space-ground conjunctions, we are in a position to present a sufficiently lucid description of a surprising event. At around 17:35 UT on 23 April 2023, a storm sudden commencement coincided with the onset of rapid, high-amplitude fluctuations in the solar wind dynamic pressure (Figure 2b); possibly indicating high-speed jets in the magnetosheath [36, 42], which are known to cause aurorae in the noon-sector [43]. Regard-

less of the cause, the dynamic pressure thereafter went through a six-fold increase, leading to a severe compression of Earth's dayside magnetosphere. This coincided with the interplanetary magnetic field settling into a stable and severely southward orientation (Figure 2a). Dayside compression events modulate wave activity [35], leading to the formation of aurorae, [44] an outcome also expected from the severely southward interplanetary magnetic field. Figures 3 and 4 in Ref. [27] demonstrate that the above expectations were largely all brought to fruition during the event under study.

During this time, diffuse aurorae appeared south of ICEBEAR's field-of-view. We expect the aurorae to have produced strong electric field perturbations on their poleward flanks [27, 45], as well as kilometer-size gradient-drift unstable structures [46], which may have seeded smaller-scale instabilities through turbulent cascade. The field enhancements powered rapidly moving radar aurorae [33, 34]. Figure 2c shows that these radar aurora motions were faster in magnitude and panel d) of that figure shows that they were also systematically tilted in an eastward direction compared to the F-region SuperDARN-Doppler speeds. That would entail E-region motions that vastly exceed the F-region drift speeds in magnitude.

III. DISCUSSION

Naïvely, the above paragraph appears to report behaviour that is diametrically opposite to the expectations of the E- and F-region interplay. For example, Figure 2 in Ref. [41] shows observations of E-region *Doppler* speeds that were limited to the local ion sound speed (400–600 m/s), while the authors simultaneously observed that the F-region drifts were twice faster. How can we account for this seeming contradiction? The answer is relatively simple. The radar aurora motions seen by ICEBEAR track moving electric field source regions, a motion that is naturally unaffected by collisions, and is 'frozen into' the geomagnetic field. [33, 34]

We are then left with what superficially resembles poleward-moving auroral forms, but, instead of moving with the magnetospheric convection on open field-lines from the cusp and into the polar cap, they move mostly eastward powered by widely distributed diffuse aurorae.

An important question remains. Why are the super-fast motions not picked up by the local SuperDARN? If the moving electric field structures are frozen into the geomagnetic field, SuperDARN should have measured the same motions (note that the SuperDARN E-region Doppler shifts, which do not reflect plasma drifts, have been removed before presenting the data in Figure 2c). However, compared to SuperDARN, ICEBEAR operates with 30 and 60 times higher spatial and temporal resolution respectively. This large discrepancy in spatio-temporal resolution is likely to have caused SuperDARN to have missed the highly transient spikes in the electric

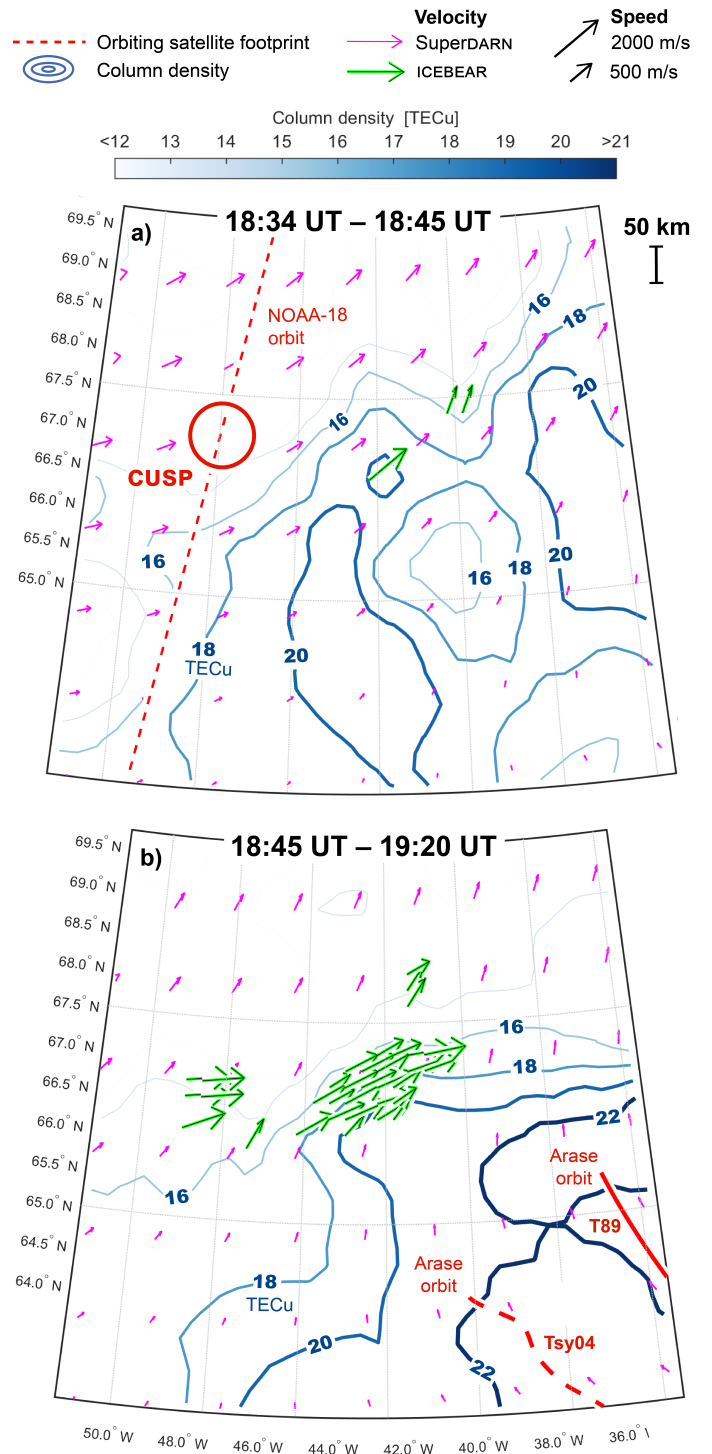


FIG. 3. ICEBEAR echo velocities in geospace are shown as green arrows, and SuperDARN global convection velocity as magenta arrows. Both are superposed on height-integrated density maps of the ionosphere (blue-colored contour lines of constant TECu). Conjunctions with the spacecraft NOAA-18 (18:35 UT – 18:40 UT on 23 April 2023) and Arase (18:50 UT – 19:20 UT) are indicated. NOAA-18 identified the location of the cusp. Some 15 minutes later, Arase saw signatures of diffuse aurorae at a location south-east of the echo region.

field. Such ‘spiky’ appearances are unsurprising. The perturbed electric fields of the auroral region are, in general, highly localized and dynamic [47–50], and a considerable Poynting flux lies “hidden”, as it were, in small-scale electric field enhancements [51].

Increased conductivities in the sunlit ionosphere should amplify (and be amplified by) the number flux of precipitating electrons [52], thereby further enhancing the perpendicular electric field at their emission altitude. The elevated conductivities also facilitate the formation of Pedersen currents, which in fact counteract the electric field enhancements, by virtue of neutralizing extant charges. However, the observed particle precipitation (Figures 2 and 3 in Ref. [27]) should increase the ratio of Hall- to Pedersen conductance [53, 54], speaking to the probability of there being observable electrojets. In this telling, the Hall drift that we observe may have appeared as the poleward portion of the pulsating aurora convection vortices predicted by Hosokawa et al. [54, 55].

The large latitudinal separation between Arase and the Hall current channels

In Figure 3 the latitudinal distance between Arase’s ionospheric footprint and the observed, turbulent Hall channels exceeds several hundred kilometers. A large distance notwithstanding, the observed particle precipitation likely covered a large region of space, as is typical for diffuse aurorae [56]. Figure 4, reproduced from Ref. [27], detail the matching temporal characteristics of the radar aurorae and the observed particle flux, with a strong Pearson correlation coefficient obtained after shifting the precipitation data backwards by 5.5 minutes, and with several peaks matching between the two timeseries. In a nutshell, the black signal in Figure 4 originated in the equatorial magnetosphere, while the red signal were measured in the E-region, and the strong correlation between the two proves a clear association. The time-lag explains the large latitudinal separation, as the active regions drifted poleward together with the magnetospheric convection.

A parallel-plate capacitor-effect

The relative positions of the observed motions with respect to the cusp itself opens up a novel perspective on poleward motions near the cusp-region. That region’s constant flux of protons (Figure 2 in Ref. [27]) would ionize the atmosphere at an altitude of around 120 km [57]. Together with the region of diffuse aurorae, which deposits negative charges, a parallel-plate capacitor momentarily forms, with strong electric fields distributing charges equatorward in the Pedersen direction. Turbulent electrojets form inside the parallel-plate capacitor, which is illustrated in Figure 1b). The effect would cause field-lines equatorward of the cusp to move

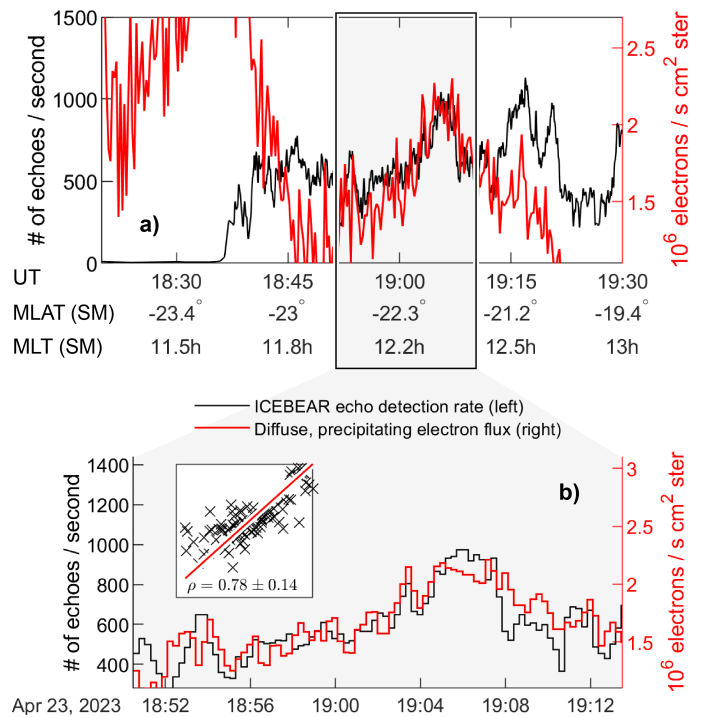


FIG. 4. Panel a): Comparison between the ICEBEAR echo detection rate (shifted 5.5 minutes forward in time and smoothed with a 16-second Savitsky-Golay filter, black, left axis) and the integrated precipitating number flux from Arase (red, right axis). The x -axes show time in UT, magnetic latitude, and magnetic local time for Arase in SM-coordinates. Panel b) enlarges a ~ 20 minute interval from Panel a), and the Pearson correlation coefficient between the two timeseries ($\rho = 0.78$) is indicated with an inset linear regression. Figure reprinted from Ref. [27] with permission.

poleward and eastward. This would transport plasma towards the open-closed field-line boundary, at which point the reconnection rate may transport the plasma into the polar cap. To determine whether there are observable islands of plasma that enter the polar cap in this way is outside the scope of the present study, and represents an independent prediction for future studies.

Closing Remarks

Traditional poleward-moving auroral forms move on open field-lines [3, 11] and their effects are felt in the F-region ionosphere [8, 12, 14]. In a similar fashion albeit in different ways, transient, turbulent electrojets can be excited equatorward of the cusp ionosphere during disturbed conditions, powered mainly by high-energy diffuse aurorae, a staple phenomenon on the dayside [21, 22, 58]. Our proposed mechanism (and the theory developed by Ref. [18]) can potentially be woven into a substantial part of the body of knowledge concerning dynamic dayside aurorae and the magnetosphere-ionosphere coupling.

Our study is based on an analysis of a single extra-

ordinary event. Similar observations may have eluded previous efforts in part due to the difficulty of observing the E-region ionosphere, which has led to a scarcity in reliable data [59]. Exacerbating this, ICEBEAR is located at auroral latitudes and is not likely to observe the cusp on a regular basis. Further studies of the phenomenon are needed, and in this regard the rich dataset analyzed in the present study may yield additional insights through modelling efforts. [60, 61]

In closing, we have observed a new, dynamic phenomenon near the ionospheric cusp, pertinent to transient energy exchanges between the turbulent magnetosheath and the dayside ionosphere on closed field-lines. The fast motions share some key characteristics with poleward-moving auroral forms, but the two phenomena have starkly different causes. Naturally, they are not mutually exclusive but can both be taken to account for observations of strong electric field modulations near the ionospheric cusp.

ACKNOWLEDGEMENTS

This work is supported in part by Research Council of Norway (RCN) grant [324859]. We acknowl-

edge the support of the Canadian Space Agency (CSA) [20SUGOICEB], the Canada Foundation for Innovation (CFI) John R. Evans Leaders Fund [32117], the Natural Science and Engineering Research Council (NSERC), the Discovery grants program [RGPIN-2019-19135], the Digital Research Alliance of Canada [RRG-4802], and basic research funding from Korea Astronomy and Space Science Institute [KASI2024185002]. Science data of the ERG (Arase) satellite were obtained from the ERG Science Center operated by ISAS/JAXA and ISEE/Nagoya University (<https://ergsc.isee.nagoya-u.ac.jp/index.shtml.en>). This includes Lv.3 MEP-e (DOI 10.34515/DATA.ERG-02003), Lv.2 PWE/OFA (DOI 10.34515/DATA.ERG-08000), Lv.2 PWE/HFA (DOI 10.34515/DATA.ERG-10000), and Lv.2 MGF (DOI 10.34515/DATA.ERG-06001). ICEBEAR 3D echo data for 2020, 2021 is published with DOI 10.5281/zenodo.7509022. SuperMAG data can be accessed at <https://supermag.jhuapl.edu/mag/>. The SymH-index from NASA's OMNI service can be accessed at <https://omniweb.gsfc.nasa.gov/>. MFI is thankful to D. Billett for stimulating discussions.

We sadly acknowledge the passing of co-author Kathryn McWilliams during the preparation of this manuscript.

-
- [1] J. W. Dungey, Interplanetary Magnetic Field and the Auroral Zones, *Physical Review Letters* **6**, 47 (1961).
 - [2] S. W. H. Cowley, TUTORIAL: Magnetosphere-Ionosphere Interactions: A Tutorial Review, Washington DC American Geophysical Union Geophysical Monograph Series **118**, 91 (2000).
 - [3] M. Saunders, The polar cusp ionosphere: A window on solar wind-magnetosphere coupling, *Antarctic Science* **1**, 193 (1989).
 - [4] G. G. Shepherd, Dayside cleft aurora and its ionospheric effects, *Reviews of Geophysics* **17**, 2017 (1979).
 - [5] Y. Ogawa, R. Fujii, S. C. Buchert, S. Nozawa, and S. Ohtani, Simultaneous EISCAT Svalbard radar and DMSP observations of ion upflow in the dayside polar ionosphere, *Journal of Geophysical Research: Space Physics* **108**, 10.1029/2002JA009590 (2003).
 - [6] H. U. Frey, D. Han, R. Kataoka, M. R. Lessard, S. E. Milan, Y. Nishimura, R. J. Strangeway, and Y. Zou, Dayside Aurora, *Space Science Reviews* **215**, 51 (2019).
 - [7] D. J. Southwood, C. J. Farrugia, and M. A. Saunders, What are flux transfer events?, *Planetary and Space Science* **36**, 503 (1988).
 - [8] K. Oksavik, J. Moen, and H. C. Carlson, High-resolution observations of the small-scale flow pattern associated with a poleward moving auroral form in the cusp, *Geophysical Research Letters* **31**, 10.1029/2004GL019838 (2004).
 - [9] G. J. Fasel, Dayside poleward moving auroral forms: A statistical study, *Journal of Geophysical Research: Space Physics* **100**, 11891 (1995).
 - [10] M. Lester, Coherent-Scatter Radar Studies of the Dayside Cusp, in *Polar Cap Boundary Phenomena*, edited by J. Moen, A. Egeland, and M. Lockwood (Springer Netherlands, Dordrecht, 1998) pp. 219–232.
 - [11] P. E. Sandholt and C. J. Farrugia, Poleward moving auroral forms (PMAFs) revisited: Responses of aurorae, plasma convection and Birkeland currents in the pre-and postnoon sectors under positive and negative IMF B_y conditions, *Annales Geophysicae* **25**, 1629 (2007).
 - [12] K. Oksavik, C. van der Meeren, D. A. Lorentzen, L. J. Baddeley, and J. Moen, Scintillation and loss of signal lock from poleward moving auroral forms in the cusp ionosphere, *Journal of Geophysical Research: Space Physics* **120**, 9161 (2015).
 - [13] S. E. Milan, M. Lester, S. W. H. Cowley, and M. Brittnacher, Convection and auroral response to a southward turning of the IMF: Polar UVI, CUTLASS, and IMAGE signatures of transient magnetic flux transfer at the magnetopause, *Journal of Geophysical Research: Space Physics* **105**, 15741 (2000).
 - [14] K. A. McWilliams, T. K. Yeoman, and S. W. H. Cowley, Two-dimensional electric field measurements in the ionospheric footprint of a flux transfer event, *Annales Geophysicae* **18**, 1584 (2000).
 - [15] P. E. Sandholt, Auroral electrodynamics at the cusp/cleft poleward boundary during northward interplanetary magnetic field, *Geophysical Research Letters* **18**, 805 (1991).
 - [16] A. Kozlovsky and J. Kangas, Motion and origin of noon high-latitude poleward moving auroral arcs on closed magnetic field lines, *Journal of Geophysical Research: Space Physics* **107**, SMP 1 (2002).
 - [17] Y.-J. J. Wu, S. B. Mende, and H. U. Frey, Simultaneous Observations of Poleward-Moving Auroral Forms at

- the Equatorward and Poleward Boundaries of the Auroral Oval in Antarctica, *Journal of Geophysical Research: Space Physics* **125**, e2019JA027646 (2020).
- [18] W. Lyatsky and D. Sibeck, Central plasma sheet disruption and the formation of dayside poleward moving auroral events, *Journal of Geophysical Research: Space Physics* **102**, 17625 (1997).
- [19] W. Lyatsky, C. Pollock, M. L. Goldstein, S. Lyatskaya, and L. Avanov, Penetration of magnetosheath plasma into dayside magnetosphere: 1. Density, velocity, and rotation, *Journal of Geophysical Research: Space Physics* **121**, 7699 (2016).
- [20] M. Spasojevic and U. S. Inan, Drivers of chorus in the outer dayside magnetosphere, *Journal of Geophysical Research: Space Physics* **115**, 10.1029/2009JA014452 (2010).
- [21] Y. Nishimura, J. Bortnik, W. Li, R. M. Thorne, B. Ni, L. R. Lyons, V. Angelopoulos, Y. Ebihara, J. W. Bonnell, O. Le Contel, and U. Auster, Structures of dayside whistler-mode waves deduced from conjugate diffuse aurora, *Journal of Geophysical Research: Space Physics* **118**, 664 (2013).
- [22] B. Ni, J. Bortnik, Y. Nishimura, R. M. Thorne, W. Li, V. Angelopoulos, Y. Ebihara, and A. T. Weatherwax, Chorus wave scattering responsible for the Earth's dayside diffuse auroral precipitation: A detailed case study, *Journal of Geophysical Research: Space Physics* **119**, 897 (2014).
- [23] B. Ni, R. M. Thorne, Y. Y. Shprits, and J. Bortnik, Resonant scattering of plasma sheet electrons by whistler-mode chorus: Contribution to diffuse auroral precipitation, *Geophysical Research Letters* **35**, 10.1029/2008GL034032 (2008).
- [24] B. Ni, R. M. Thorne, N. P. Meredith, R. B. Horne, and Y. Y. Shprits, Resonant scattering of plasma sheet electrons leading to diffuse auroral precipitation: 2. Evaluation for whistler mode chorus waves, *Journal of Geophysical Research: Space Physics* **116**, 10.1029/2010JA016233 (2011).
- [25] X. Fang, C. E. Randall, D. Lummerzheim, W. Wang, G. Lu, S. C. Solomon, and R. A. Frahm, Parameterization of monoenergetic electron impact ionization, *Geophysical Research Letters* **37**, 10.1029/2010GL045406 (2010).
- [26] G. W. Prölss, Absorption and Dissipation of Solar Radiation Energy, in *Physics of the Earth's Space Environment: An Introduction*, edited by G. W. Prölss (Springer, Berlin, Heidelberg, 2004) pp. 77–157.
- [27] M. Ivarsen, Y. Jin, D. Huyghebaert, Y. Miyashita, J.-P. St.-Maurice, G. Hussey, K. McWilliams, S. Kasahara, D. Sibeck, K. Song, P. Jayachandran, B. Dan, L. Clausen, S. Yokota, Y. Miyoshi, Y. Kasahara, I. Shinohara, and A. Matsuoka, Transient, Turbulent Hall Currents in the Sunlit Terrestrial Ionosphere (2024).
- [28] N. E. Papitashvili and J. H. King, OMNI Hourly Data Set (2020).
- [29] D. L. Hysell, The Radar Aurora, in *Auroral Dynamics and Space Weather* (American Geophysical Union (AGU), 2015) Chap. 14, pp. 191–209.
- [30] D. Huyghebaert, G. Hussey, J. Vierinen, K. McWilliams, and J.-P. St.-Maurice, ICEBEAR: An all-digital bistatic coded continuous-wave radar for studies of the E region of the ionosphere, *Radio Science* **54**, 349 (2019).
- [31] D. T. Farley, A plasma instability resulting in field-aligned irregularities in the ionosphere, *Journal of Geophysical Research* (1896-1977) **68**, 6083 (1963).
- [32] O. Buneman, Excitation of Field Aligned Sound Waves by Electron Streams, *Physical Review Letters* **10**, 285 (1963).
- [33] M. F. Ivarsen, J.-P. St.-Maurice, G. C. Hussey, D. R. Huyghebaert, and M. D. Gillies, Point-cloud clustering and tracking algorithm for radar interferometry, *Physical Review E* **110**, 045207 (2024).
- [34] M. F. Ivarsen, J.-P. St.-Maurice, D. R. Huyghebaert, M. D. Gillies, F. Lind, B. Pitzel, and G. C. Hussey, Deriving the Ionospheric Electric Field From the Bulk Motion of Radar Aurora in the E-Region, *Journal of Geophysical Research: Space Physics* **129**, e2024JA033060 (2024).
- [35] J.-H. Li, X.-Z. Zhou, S. Wang, Z.-Y. Liu, Q.-G. Zong, S.-T. Yao, A. V. Artemyev, Y. Omura, L. Li, C. Yue, and Q.-Q. Shi, Bow Shock Ripples and Their Modulation of Whistler Wave Packets: MMS Observations, *Geophysical Research Letters* **51**, e2024GL111590 (2024).
- [36] E. Krämer, F. Koller, J. Suni, A. T. LaMoury, A. Pöppelwerth, G. Glebe, T. Mohammed-Amin, S. Raptis, L. Vuorinen, S. Weiss, N. Xirogiannopoulou, M. Archer, X. Blanco-Cano, H. Gunell, H. Hietala, T. Karlsson, F. Plaschke, L. Preisser, O. Roberts, C. Simon Wedlund, M. Temmer, and Z. Vörös, Jets Downstream of Collisionless Shocks: Recent Discoveries and Challenges, *Space Science Reviews* **221**, 4 (2024).
- [37] G. Vichare, A. Bhaskar, R. Rawat, V. Yadav, W. Mishra, D. Angchuk, and A. K. Singh, Low-Latitude Auroras: Insights from 23 April 2023 Solar Storm (2024), arXiv:2405.08821 [astro-ph, physics:physics].
- [38] J. R. Souza, P. Dandenault, A. M. Santos, J. Riccobono, M. A. Migliozzi, S. Kapali, R. B. Kerr, R. Mesquita, I. S. Batista, Q. Wu, A. A. Pimenta, J. Noto, J. Huba, L. Peres, R. Silva, and C. Wrasse, Impacts of Storm Electric Fields and Traveling Atmospheric Disturbances Over the Americas During 23–24 April 2023 Geomagnetic Storm: Experimental Analysis, *Journal of Geophysical Research: Space Physics* **129**, e2024JA032698 (2024).
- [39] E. Aa, S.-R. Zhang, S. Zou, W. Wang, Z. Wang, X. Cai, P. J. Erickson, and A. J. Coster, Significant Midlatitude Bubble-Like Ionospheric Super-Depletion Structure (BLISS) and Dynamic Variation of Storm-Enhanced Density Plume During the 23 April 2023 Geomagnetic Storm, *Space Weather* **22**, e2023SW003704 (2024).
- [40] E. Nielsen and K. Schlegel, A first comparison of STARE and EISCAT electron drift velocity measurements, *Journal of Geophysical Research* **88**, 5745 (1983).
- [41] J. C. Foster and P. J. Erickson, Simultaneous observations of E-region coherent backscatter and electric field amplitude at F-region heights with the Millstone Hill UHF Radar, *Geophysical Research Letters* **27**, 3177 (2000).
- [42] M. O. Archer, H. Hietala, M. D. Hartinger, F. Plaschke, and V. Angelopoulos, Direct observations of a surface eigenmode of the dayside magnetopause, *Nature Communications* **10**, 615 (2019).
- [43] H.-X. Qiu, D.-S. Han, R. Shi, and J. Liu, Magnetosheath High-Speed Jet Drives Multiple Auroral Arcs Near Local Noon, *AGU Advances* **5**, e2024AV001197 (2024).
- [44] Q. Q. Shi, X.-C. Shen, A. M. Tian, A. W. Degeling, Q. Zong, S. Y. Fu, Z. Y. Pu, H. Y. Zhao, H. Zhang, and S. T. Yao, Magnetosphere Response to Solar Wind Dynamic Pressure Change, in *Dayside Magnetosphere In-*

- teractions* (American Geophysical Union (AGU), 2020) Chap. 5, pp. 77–97.
- [45] M. F. Ivarsen, D. R. Huyghebaert, M. D. Gillies, J.-P. St-Maurice, D. R. Themens, M. Oppenheim, B. J. Gustavsson, D. Billett, B. Pitzel, D. Galeschuk, E. Donovan, and G. C. Hussey, Turbulence Around Auroral Arcs, *Journal of Geophysical Research: Space Physics* **129**, e2023JA032309 (2024).
- [46] R. A. Greenwald, Diffuse radar aurora and the gradient drift instability, *Journal of Geophysical Research* (1896-1977) **79**, 4807 (1974).
- [47] B. S. Lanchester, K. Kaila, and I. W. McCrea, Relationship between large horizontal electric fields and auroral arc elements, *Journal of Geophysical Research: Space Physics* **101**, 5075 (1996).
- [48] H. J. Opgenoorth, I. Hägström, P. J. S. Williams, and G. O. L. Jones, Regions of strongly enhanced perpendicular electric fields adjacent to auroral arcs, *Journal of Atmospheric and Terrestrial Physics The Fourth International EISCAT Workshop*, **52**, 449 (1990).
- [49] S. Tuttle, B. Lanchester, B. Gustavsson, D. Whiter, N. Ivchenko, R. Fear, and M. Lester, Horizontal electric fields from flow of auroral O^+ (2P) ions at sub-second temporal resolution, *Annales Geophysicae* **38**, 845 (2020).
- [50] P. Krcelic, R. C. Fear, D. Whiter, B. Lanchester, and N. Brindley, Variability in the Electrodynamics of the Small Scale Auroral Arc, *Journal of Geophysical Research: Space Physics* **129**, e2024JA032623 (2024).
- [51] D. D. Billett, K. A. McWilliams, I. P. Pakhotin, J. K. Burchill, D. J. Knudsen, and C. J. Martin, High-Resolution Poynting Flux Statistics From the Swarm Mission: How Much Is Being Underestimated at Larger Scales?, *Journal of Geophysical Research: Space Physics* **127**, e2022JA030573 (2022).
- [52] K. Liou, P. T. Newell, and C.-I. Meng, Seasonal effects on auroral particle acceleration and precipitation, *Journal of Geophysical Research: Space Physics* **106**, 5531 (2001).
- [53] C. Senior, R. M. Robinson, and T. A. Potemra, Relationship between field-aligned currents, diffuse auroral precipitation and the westward electrojet in the early morning sector, *Journal of Geophysical Research: Space Physics* **87**, 10469 (1982).
- [54] K. Hosokawa, Y. Ogawa, A. Kadokura, H. Miyaoka, and N. Sato, Modulation of ionospheric conductance and electric field associated with pulsating aurora, *Journal of Geophysical Research: Space Physics* **115**, 10.1029/2009JA014683 (2010).
- [55] K. Hosokawa, S. E. Milan, M. Lester, A. Kadokura, N. Sato, and G. Bjornsson, Large flow shears around auroral beads at substorm onset, *Geophysical Research Letters* **40**, 4987 (2013).
- [56] Y. Nishimura, M. R. Lessard, Y. Katoh, Y. Miyoshi, E. Grono, N. Partamies, N. Sivadass, K. Hosokawa, M. Fukizawa, M. Samara, R. G. Michell, R. Kataoka, T. Sakanoi, D. K. Whiter, S.-i. Oyama, Y. Ogawa, and S. Kurita, Diffuse and Pulsating Aurora, *Space Science Reviews* **216**, 4 (2020).
- [57] X. Fang, D. Lummerzheim, and C. H. Jackman, Proton impact ionization and a fast calculation method, *Journal of Geophysical Research: Space Physics* **118**, 5369 (2013).
- [58] H. Feng, D. Wang, D. Guo, Y. Y. Shprits, D. Han, S. Teng, B. Ni, R. Shi, and Y. Zhang, Lower Band Chorus Wave Scattering Causing the Extensive Morningside Diffuse Auroral Precipitation During Active Geomagnetic Conditions: A Detailed Case Study, *Journal of Geophysical Research: Space Physics* **129**, e2023JA032240 (2024).
- [59] M. Palmroth, M. Grandin, T. Sarris, E. Doornbos, S. Tourgaidis, A. Aikio, S. Buchert, M. A. Clilverd, I. Dandouras, R. Heelis, A. Hoffmann, N. Ivchenko, G. Kervalishvili, D. J. Knudsen, A. Kotova, H.-L. Liu, D. M. Malaspina, G. March, A. Marchaudon, O. Marghitu, T. Matsuo, W. J. Miloch, T. Moretto-Jørgensen, D. Mpaloukidis, N. Olsen, K. Papadakis, R. Pfaff, P. Pirnaris, C. Siemes, C. Stolle, J. Suni, J. van den IJssel, P. T. Verronen, P. Visser, and M. Yamauchi, Lower-thermosphere-ionosphere (LTI) quantities: Current status of measuring techniques and models, *Annales Geophysicae* **39**, 189 (2021).
- [60] M. Wiltberger, V. Merkin, B. Zhang, F. Toffoletto, M. Oppenheim, W. Wang, J. G. Lyon, J. Liu, Y. Dimant, M. I. Sitnov, and G. K. Stephens, Effects of electrojet turbulence on a magnetosphere-ionosphere simulation of a geomagnetic storm, *Journal of Geophysical Research: Space Physics* **122**, 5008 (2017).
- [61] Q. Wu, W. Wang, D. Lin, C. Huang, and Y. Zhang, Penetrating Electric Field Simulated by the MAGE and Comparison With ICON Observation, *Journal of Geophysical Research: Space Physics* **127**, e2022JA030467 (2022).